The *Prrx1* limb enhancer marks an adult population of injury-responsive, multipotent dermal fibroblasts

Joshua D. Currie[1,2], Lidia Grosser[1,3], Prayag Murawala[1,3], Maritta Schuez[1], Martin Michel[1], Elly M. Tanaka[1,3], Tatiana Sandoval-Guzmán[1]*

1. CRTD - Center for Regenerative Therapies Dresden, Technische Universität Dresden, Fetscherstrasse 105, 01307 Dresden, Germany
2. Department of Cell and Systems Biology, University of Toronto, 25 Harbord Street, M5S 3G5 Toronto, Canada
3. Research Institute for Molecular Pathology (IMP), Vienna Biocenter (VBC), Campus-Vienna-Biocenter 1, 1030 Vienna, Austria

* Author to whom correspondence should be addressed: tatiana.sandoval_guzman@tu-dresden.de

Running Title: *Prrx1*-enhancer labels injury-responsive fibroblasts

Keywords: Lineage tracing, dermal fibroblast, wound healing, limb progenitor.

Competing Interests:

The authors declare no competing financial interests.

Summary

The heterogeneity of adult tissues has been posited to contribute toward the loss of regenerative potential in mammals. Here we characterize an adult population of dermal fibroblasts that maintain expression of a *Prrx1* enhancer which originally marked mesenchymal limb progenitors. *Prrx1* enhancer-positive cells (Prrx1^{enh+}) make up a small subset of adult dermal cells (~0.2%) and reside mainly within specific dermal perivascular and hair follicle niches. Upon injury, however, Prrx1^{enh+} cells readily migrate into the wound bed and amplify on average 16-fold beyond their uninjured numbers. Additionally, Prrx1^{enh+} cells emigrate out of their dermal niches following wounding and contribute to subcutaneous tissue. Prrx1^{enh+} cells are uniquely injury-responsive and do not contribute to tissue homeostasis or enriched by neonatal-like Wnt signaling. Prrx1^{enh+} cells represent a potent regenerative cell population that, despite being a meager minority in adult skin, demonstrate the potential to tip the balance of mammalian wound healing toward scar-free healing.

Introduction

In the search for therapies that enhance wound healing or reduce fibrosis, cellular heterogeneity has emerged as an added layer of complexity that profoundly shapes the outcome of wound responses (Driskell et al. 2013, Nature). The heterogeneity of connective tissue fibroblasts has been of particular importance, since these cells are the main actors during wound healing to produce either scar-free healing or unresolved fibrotic scars (Gurtner, Werner, Barrandon, & Longaker, 2008). Central to this idea, is that mixed populations of cells may carry intrinsic differences in their response to wound-related signals or their capacity to reconstitute all the structures of the intact organ.

To disentangle fibroblast heterogeneity, several groups have identified fibroblast subgroups by a single or battery of molecular markers. Cells derived from Engrailed-1 embryonic lineage (Rinkevich et al., 2015) or adult cells with *Gli-1*$^{+}$ expression have been shown to contribute to wound fibrosis (Kramann et al., 2014), while expansion of BLIMP1^{+} dermal cells can support de novo hair follicle formation during wound repair (Kretzschmar et al., 2014). Ideally, such categorization would distinguish subpopulations, with higher regenerative or differentiation potential, that could be analyzed in isolation from fibrosis-associated cells. The final goal, would be to amplify and recruit such a regenerative population during wound repair, or inversely, deter fibrotic cells from making contributions to wound healing.

The embryonic origin and site of injury is an important consideration of wound-related cells. The majority of work defining fibroblast heterogeneity and contribution to wounding has been performed by wounding of dorsal back skin. Wounds made in dorsal skin are experimentally preferable as they can be easily cleaned and allow for large wounds (greater than 4mm) that can be splinted to avoid wound contraction. Despite these advantages, the makeup of dermal cells within back skin is primarily derived from paraxial mesoderm, which neglects a large majority of mesenchymal cells of other embryonic origins that may display differential plasticity and response to wounding.

To identify adult cells that retain a progenitor-like ability to participate in tissue formation, we looked at molecular markers that are present during development or in highly regenerative contexts such as salamander limb regeneration. One such marker is the transcription factor paired-related homeobox 1 (*Prrx1* or *Prx1*), an early marker of lateral plate mesoderm (LPM) that labels progenitors of nascent limb skeleton and soft connective tissue of the flank and limb. Additionally, *Prrx1* is upregulated following salamander limb amputation (Satoh, Gardiner, Bryant,

& Endo, 2007) as well as in anuran limb regeneration (Suzuki, Satoh, Ide, & Tamura, 2005). Transgenic mouse models of *Prrx1* activity have relied on a specific enhancer that encompasses approximately 2.4kb upstream of the transcriptional start site (Logan et al., 2002). The enhancer drives LacZ or Cre recombinase expression in embryonic lateral soft connective tissue, portions of craniofacial mesenchyme, and limb skeleton and connective tissue. Whether PRRX1 protein (PRRX1^{+}) or enhancer activity (Prrx1^{enh+}) remain postnatally has not been fully determined. A recent report has implicated a population of PRRX1^{+} cells in the regeneration of calvarial bone (Wilk et al., 2017). This lead us to hypothesize that *Prrx1*-positive cells in other postnatal tissues might also have a role in wound healing and repair.

Here we employ an inducible Prrx1-enhancer (Prrx1^{enh+}) CreERT transgenic line to lineage trace dermal cells in postnatal and adult mice. We found that adult Prrx1^{enh+} cells remain confined to tissues that were formed by embryonic, Prrx1-postive anlages, namely lateral plate mesoderm (LPM) and craniofacial mesenchyme. Although the majority of mesenchymal cells in the limb bud are Prrx1^{enh+}, the total number of Prrx1^{enh+} cells drops dramatically after birth, making up roughly 0.1% of mesenchymal cells within the adult epidermis. In contrast to the majority of mesenchymal dermal cells that are positive for PRRX1 protein as detected by antibody staining, Prrx1^{enh+} cells are retained in specific dermal compartments. Prrx1^{enh+} cells do not participate in tissue maintenance. Instead, these cells exhibit a robust response to wounding, amplifying in the wound bed 2-16 fold over their numbers in uninjured skin. Prrx1^{enh+} cells do not express high levels of fibrotic myofibroblast markers, and contribute to a range of differentiated structures both within the dermis as well as subcutaneous tissues after injury. This is in contrast to distinct fibroblast populations traced by *Col1a2* enhancer, which do not exhibit the same injury-specific properties. Finally, we hypothesized that an embryonic microenvironment might be necessary to enrich for Prrx1^{enh+} cells. Therefore, we challenged the adult skin to a neonatal state with sustained Wnt signaling to enhance the Prrx1^{enh+} population. We found that re-activation of neonatal levels of Wnt signaling fails to amplify the number of Prrx1^{enh+} cells inside the wound bed or in uninjured skin. Taken together, our results highlight a small population of cells in adult dermis that retain activation of an embryonic enhancer, are uniquely tuned to respond to injury, and have an expanded contribution during wound healing.

Results

PRRX1 in developing limb and adult connective tissue

Prrx1 was originally characterized as a progenitor marker of limb skeleton and soft connective tissue using a combination of *in situ* hybridization and Cre recombinase and LacZ transgenic mice (Chesterman, Gainey, Varn, Peterson, & Kern, 2001). However, a precise timeline of protein expression at both embryonic and postnatal timepoints had not been fully investigated. To do this, we used a polyclonal antibody that was generated against the N-terminal amino acids 1-101 of the axolotl (*Ambystoma mexicanum*) PRRX1 protein that shares broad conservation with other vertebrate homologs (Oliveira et al., 2017). We validated the specificity of our antibody by comparing staining of previously reported anti-rat PRRX1 antibody (Higuchi et al., 2013). We found matching patterns of expression in adjacent sections of the developing limb between our PRRX1 antibody, confirming the specificity of our antibody in mouse. (Fig. 1 A and B). By immunohistochemistry, PRRX1$^+$ cells were detected in limb bud and lateral plate as early as E9.5, where most mesenchymal cells are positive (Figure 2 A). At this stage, expression of the protein is homogenous in what is considered the beginning of the budding phase. At E10.5 the limb bud is defined and protruding from the body flank. PRRX1$^-$ cells exist at the junction of the arm, possibly from colonizing endothelial and myogenic precursors (Figure 2 B). At E12.5, cartilage condensations become evident, with cells within the condensate down regulate *Prrx1* expression. However, most mesenchymal cells still remain PRRX1$^+$ (Figure 2 C). During development we found that expression of PRRX1 protein was also detected in tissues outside the limb as reported previously using in situ hybridization (Leussink et al., 1995). These include tissues from mesodermal origin such as back skin, rib cartilage, trachea, and from neural crest origin such as cranial mesenchyme.

At E16.5, clear PRRX1$^+$ and PRRX1$^-$ zones are visible in the limb, although most connective tissue cells are still PRRX1$^+$ (Figure 2 D). We further investigated if PRRX1 remains in postnatal tissue or if its expression is restricted to embryonic and neonatal stages. In postnatal day 3 (P3) PRRX1$^+$ cells persist abundantly in dermis (Figure 2 E). Since PDGFRα has been previously suggested as a pan marker of dermal fibroblasts (Driskell et al., 2013), we used the *Pdgfrα-H2B-EGFP* transgenic mouse to quantify the overlap of PRRX1$^+$ in adult mesenchymal dermal tissue (Figure 2 F). We found that in 7 week-old mice 12,7% ± 4,1 (n=6) of total PRRX1$^+$ cells are PDGFRα$^-$. Conversely, 22,8% ± 10,1 of the total PDGFRα$^+$ cells are PRRX1$^-$ (Figure 2 G-H). This result agrees with data from Rinkevich et al., who found that a considerable percentage of *Engrailed-1* lineage fibroblasts do not express PDGFRα (Rinkevich et al., 2015). Since neither PRRX1 or PDGFRα encompassed the full complement of mesenchymal cells and PDGFRα is

also expressed in non-mesenchymal lineages such as megakaryocytes and platelets (Demoulin & Montano-Almendras, 2012; Ye et al., 2010), we decided to use PRRX1 antibody (PRRX1$^+$ cells) to demarcate a broad mesenchymal population in the dermis.

In summary, we found that PRRX1 protein delineates mesenchymal progenitors in the developing limb, and the expression of PRRX1 protein persists into adulthood. The cell population that express PRRX1 covers a large but not complete percentage of the mesenchymal cells of the dermis that mostly overlaps with PDGFRα^+ mesenchymal cells.

The *Prrx1* enhancer labels embryonic mesenchymal progenitor cells and small subsets of mesenchymal cells in the adult dermis

To trace the fate of PRRX1 cells in homeostasis and injury, we generated transgenic mice expressing a nuclear teal fluorescent protein (TFP) and Cre-ERT under the control of the 2.4kb *Prrx1* enhancer element as described previously (Logan et al., 2002). We crossed the *Prrx1 enhancer-CreER-T2A-mTFPnls* mice with *Rosa-CAG-loxP-stop-loxP-TdTomato* mice (referred to as *Prrx1enh-CreER;LSL-tdTomato*)(Figure 3 A), allowing us to trace the fate of *Prrx1* enhancer-positive cells (Prrx1^{enh+}) upon tamoxifen administration. A single low dose of tamoxifen (1mg, gavage) to gestating mothers to elicit conversion in E10.5 embryos, yielded labeling of Prrx1^{enh+} cells in a majority of limb bud cells, facial mesenchyme, and inter-limb flank (Figure 3 B). In postnatal and juvenile mice, the conversion of the *Prrx1* enhancer was vastly reduced such that even after five high concentration doses of tamoxifen (5mg, gavage), only a small subset of cells was visible within the dermis and scattered in other connective tissues of the limb (Figure 3 E). Three weeks after tamoxifen administration, labelled Prrx1^{enh+} cells were found primarily within two specialized dermal niches: the hair follicle dermal papillae (dp) 84% (Figure 3 C) and in the perivascular space (Figure 3 D). Prrx1^{enh+} cells were also occasionally found in the dermal sheath of hair follicles and in papillary dermis. We confirmed in tissue sections that all Prrx1^{enh+} cells in the adult dermis were also PRRX1$^+$. Prrx1^{enh+} cells made up just 0.22% ± 0.75 SD (n= 6) of the total PRRX1$^+$ mesenchymal cells in the adult limb dermis. Likewise, dissociation of the dermis and FAC sorting revealed that approximately 0.48% ± 0.33 SD, of dermal cells were tdTOMATO$^+$ (Figure 3 F). We also confirmed that the higher conversion dose required in young adult mice was not due to inaccessibility to tamoxifen, since administration either intraperitoneally or intravenously, yielding the same number of cells converted (data not shown). Furthermore, we dissociated dermal cells from *Prrx1enh-CreER;LSL-tdTomato* mice, to allow *in vitro* conversion of

Prrx1^{enh+} and found no difference in the percentage of converted cells to that of intact dermis (data not shown). Thus, the Prrx1^{enh+} marks a broad embryonic population that reaches its peak during limb formation but the number of cells that can be converted rapidly declines after birth. In adulthood, it demarks a narrow subset of mesenchymal cells.

***Prrx1* enhancer cells are injury-responsive and vastly amplify upon limb full-thickness skin wounding**

We were curious if these limited Prrx1^{enh+} cells in the adult mouse retained embryonic-like properties that could contribute positively to repair and regeneration. Previously, the mouse *Prrx1* enhancer was shown to be active during wound healing and spike formation in Xenopus (Suzuki, Satoh, Ide, & Tamura, 2007), but absent in wound healing of mouse back skin (Yokoyama et al., 2011), the predominant experimental paradigm for skin healing in the mouse. Although PRRX1 protein is present in dermal cells of back skin, we could detect no more than one or two Prrx1^{enh+} cells in multiple sections of at least 4mm expanding along the back (n=10 animals). The lack of enhancer positive cells in back skin remained true after tamoxifen administration in embryos, adult mice, or after injury (Figure 4 A).

Given that the *Prrx1* enhancer marks limb progenitors, and fibroblasts are known to carry unique positional information based on their location in different body parts, we decided to lineage trace Prrx1^{enh+} cells in a limb full-thickness skin injury model. We performed 2mm full thickness skin wounds in the upper limbs of *Prrx1enh-CreER;LSL-tdTomato*. Mice were wounded three weeks after the last administration of tamoxifen to prevent recombination during wound healing. In contrast to back skin wounds, it was not possible to splint limb skin wounds. A semi-occlusive bandage (Tegaderm 3M) was applied for the first 48-62 hours to prevent infection. This bandage only mildly impedes wound contraction that is characteristic of skin wounds in rodents. Fourteen days post wounding (14 dpw), animals were sacrificed and the wounded and contralateral limb were compared for the percentage of Prrx1^{enh+} (tdTOMATO^{+}) cells. At low magnification there was already an obvious amplification of Prrx1^{enh+} cells within the wound bed compared with the adjacent wound margin and contralateral limb (Figure 5 A, B). Within 1mm^2 cross sections of the wound (Figure 5 D), despite an increased density of mesenchymal PRRX1^{+} cells, the percentage of labeled Prrx1^{enh+} cells were on average 16.46-fold increased (±12.58 SD, P = 0015) over the uninjured contralateral dermis (Figure 5 C). This is an increase of Prrx1^{enh+} from 0.37 % ±0.2 SD to 5.76 % ± 3.8 SD of the total PRRX1^{+}. During the injury response, Prrx1^{enh+} cells were not

necessarily associated to blood vessels (Figure 5 E), but primarily within the upper or papillary dermis. This result was confirmed in three independent experiments.

***Prrx1*-enhancer cells contribute to a host of non-native subcutaneous tissue compartments and do not contribute to tissue homeostasis.**

When collecting skin for tissue processing, we observed a concentration of Prrx1^{enh+} positive cells in sub cutaneous connective tissue surrounding the muscle immediately under the wounded skin (Figure 5 F, G). We found that Prrx1^{enh+} cells were located within fascia, loose connective tissue and adipose tissue. We confirmed the contribution to adipose tissue by co-staining Prrx1^{enh+} with a PERILIPIN antibody (Figure 5 H). In our experimental layout, tamoxifen is administered 5 weeks prior to tissue collection and recombination labels only a dispersed, small subset of the PRRX1^{+} cells in all connective tissue types of the unwounded or contralateral limb. This suggests that upon injury, labeled dermal-associated cells migrate from the dermis and take up residence in subcutaneous tissue where they contribute to diverse tissue types such as adipose tissue. After 4 weeks, when the 2 mm wound is resolved, and cellular content is decreased, Prrx1^{enh+} cells remain in the wound bed (Figure 5 I) where they re-acquire an association with blood vessels (Figure 5 J). The number of Prrx1^{enh+} cells in the wound after 4 weeks remains elevated compared to contralateral uninjured skin by 11.48-fold increase (± 4.1 SD)(n=6).

The high number of Prrx1^{enh+} in the wound suggests that cells that have an active enhancer under homeostatic conditions readily migrate into the wound bed and proliferate relative to other PRRX1^{+} cells. We wondered if the homeostatic expression of the Prrx1 enhancer is retained by Prrx1^{enh+} cells during the wound healing process. We administered tamoxifen 5 days post wounding (5 dpw), and collected the wound tissue at 14 days post wounding. In contrast to the recalcitrant recombination observed under uninjured conditions, only one dose of tamoxifen during the wound healing process was sufficient to convert a comparable number of Prrx1^{enh+} cells to the traced preconverted cells reported above. One dose of tamoxifen at 5dpw converts 5.1% ± 2.3 SD (n=4) Prrx1^{enh+} cells, versus 5.76 % ± 3.8 SD of Prrx1^{enh+} cells in mice that received 5 doses of tamoxifen in intact skin and then wounded. This suggest that Prrx1^{enh+} cells maintain *Prrx1* enhancer activity at potentially higher levels during wound-related migration and proliferation. Thus, we concluded that the postnatal population of Prrx1^{enh+} is a subset of the broad PRRX1^{+} population that is uniquely tuned to respond and amplify in specific response to injury.

An open question was if cells expressing the *Prrx1* enhancer at late embryonic and early postnatal periods would have a role in building and maintaining adult tissue. We administered tamoxifen perinatally and examined if Prrx1^{enh+} cell number would increase over time and in a clonal manner in specific dermal niches (Figure 6 A). We found that although the number of cells converted perinatally is higher than in adult, no clonal expansion was observed after 6 months (Figure 6 B). The same result was obtained when recombination was induced in 7 week-old mice and tissue was collected one year later (Figure 6 C, D). These results underscore the participation of Prrx1^{enh+} in injury and not in normal tissue turnover.

Prrx1 enhancer cells do not amplify in response to sustained activation of canonical Wnt pathway.

Because we observed a drop in Prrx1^{enh+} labeling shortly after birth, we wondered if the neonatal environment of the dermis was necessary to retain or enrich for enhancer positive cells. Previous reports have shown that elevated levels of Wnt signaling can re-establish such an embryonic-like skin environment. The *K14**ΔN**β-cateninER* transgenic line expresses an active form of *β*-catenin fused to the estrogen receptor under the *keratin 14* (K14) promoter. Upon tamoxifen administration, the *β-catenin-ER* fusion translocates to the nucleus and activates downstream Wnt pathway genes in keratinocytes. The sustained activation of Wnt/*β*-catenin signaling results in expansion of dermal layers, growth of existing hair follicles and ectopic hair follicle formation (Collins, Kretzschmar, & Watt, 2011). In addition, sustained Wnt/ *β*-catenin signaling has been shown to play a key role in fibroblast fate and differentiation (Mastrogiannaki et al., 2016) and wound healing (Shi et al., 2015). The effect of epidermal Wnt/ *β*-catenin on dermal layers includes extensive fibroblast proliferation and ECM remodeling, therefore we set out to investigate the response of Prrx1^{enh+} to this pathway. We used a triple transgenic mouse *K14**ΔN**β-cateninER;Prrx1enh-CreER;LSL-tdTomato*. We produce wounds in the limbs of mice that had received tamoxifen and collected tissue at 14 days post wounding. Although we observed hair follicle growth and ectopic follicle formation, consistent with the transient activation of *β*-catenin shown by Collins et al., (Collins et al., 2011), we observed no change in the number of Prrx1^{enh+} cells in intact skin (Figure 6 E) or in the wound bed in two independent experiments. This suggests

that the adult levels and maintenance of Prrx1^{enh+} cells as well as their migration and proliferation during wounding is not due to sustained activation of Wnt/β-catenin signaling.

***Col1a2* enhancer cells do not amplify upon limb full-thickness skin wounding**

An important question to address was if other subpopulations of dermal cells would also amplify in response to injury in a similar manner as Prrx1^{enh+} cells. To address this, we used a transgenic mouse expressing inducible CreER under the control of a 17-kb fragment of the *Col1a2* upstream enhancer. This transgenic mouse has been used previously as a reporter of wound healing in dorsal wounds (Higashiyama et al., 2011; Rajkumar et al., 2006). We crossed the *Col1a2 enhancer-CreER* mice with a *Rosa-CAG-loxP-stop-loxP-TdTomato* mice (referred to as *Col1a2enh-CreER;LSL-tdTomato*). Similar to the experiments described above, we administered tamoxifen 3 weeks before wounding. We quantified tdTOMATO^{+} cells as the marker for Col1a2^{enh+} in contralateral and wound tissue (Figure 7 A, B). In uninjured tissue Col1a2^{enh+} cells labeled dermal fibroblasts as well as portions of surface and interfollicular epithelia. No difference was found in the percentage of Col1a2^{enh+} cells among the total of mesenchymal PRRX1^{+} cells, in injured and intact skin (Figure 7 D). In contrast to Prrx1^{enh+} cells, mesenchymal Col1a2^{enh+} cells were not associated with blood vessels (Figure 7 C) in intact or wounded skin. Col1a2^{enh+} epithelial cells did respond to superficial injury caused by hair clipping in preparation for wounds. Labeled cells were found in the inter-follicular space and this was observed in sections and in low magnification images of the skin surrounding the wound (dashed oval in Figure 7 F). Since epidermal cells are PRRX1^{-}, these cells were excluded from our quantification. In contrast to Prrx1^{enh+} cells, we found no enrichment of positive dermal cells within the wound bed or in the subcutaneous space under the wounds (Figure 7 G, H). In fact, there was a small depletion of Col1a2^{enh+}/PRRX^{+} within the wound 21 days after injury. This suggests that the dermal cells labeled by Col1a2^{enh+} have a muted response to injury and may be slightly displaced by other subpopulations including Prrx1^{enh+} cells.

Discussion

A prevalent hypothesis is that the increased complexity and heterogeneity of cell and tissue types in mammals has been gained at the expense of regenerative abilities. This hypothesis is not mutually exclusive to the idea that some cells may have retained regenerative capacities, but are unable or diverted toward fibrotic wound resolution. We hypothesized that such regenerative cell populations could be identified if they retain markers of embryonic progenitors. In line with that, we identified one such subpopulation of connective tissue cells, the primary drivers of scar formation, that maintain the activity of an embryonic enhancer of limb progenitors, paired-related homeobox protein 1 (*Prrx1*). The *Prrx1* enhancer that has been previously described as sufficient to drive tissue-specific expression of a transgene embryonically and postnatally (Martin & Olson, 2000).

We created an inducible Cre line using this regulatory element to answer the question if such a progenitor marker might remain active in adult tissue, and if positive cells would contribute to tissue homeostasis and injury.

Our results show firstly, that by immunohistochemistry PRRX1 protein is located in connective tissue progenitors of the developing limb and expressed in a vast proportion of adult connective tissue cells. During limb development, the enhancer-driven recombination in *Prrx1enh-CreER;LSL-tdTomato* recapitulates protein (PRRX1) expression. In contrast, in postnatal animals, Prrx1^{enh+} cells demark a small population of cells from the broad mesenchymal PRRX1 population. Prrx1^{enh+} cells in the adult dermis are mainly retained in two specific niches, as perivascular cells and within the dermal papilla of the hair follicle. Dissociated cells exposed to high concentrations of Tamoxifen to induce recombination do not increase the percentage of cells recombined, suggesting that these cells are stably determined within fibroblast populations of the postnatal skin.

Secondly, upon injury, Prrx1^{enh+} migrate to the wound bed, contribute to different tissues and remain there during the resolving phase of the wound. This plasticity and cell amplification appear to be injury specific, as extended lineage tracing of Prrx1^{enh+} cells during tissue homeostasis yielded no increase in the numbers of positive cells. Superficial scratches from self-grooming also increase the number of Prrx1^{enh+} in dermis. The ability to contribute to foreign subcutaneous tissues seems unique to Prrx1^{enh+} cells, as Col1a2^{enh+} cells did not exhibit the same contribution during wound repair.

Finally, we found that sustained Wnt signaling to mimic dermal neonatal state did not expand the number Prrx1^{enh+} cells in resting tissue or enhance their response to injury.

Prrx1 has been shown to be a marker necessary for maintaining stemness in adult hippocampal tissue (Shimozaki, Clemenson, & Gage, 2013). We hypothesized that cells expressing *Prrx1* would contribute to wound repair by either providing daughter cells that would differentiate and directly contribute to structuring the wound, or by supplying factors that modulate healing.

As a marker of regenerative progenitors, *Prrx1* upregulation has been viewed as a stereotypical step in the formation of the proliferative blastema during salamander limb regeneration (Satoh et al., 2007) . Recent lineage tracing in the axolotl showed that Prrx1^{enh+} cells are multipotent cells that can regenerate skeleton and soft connective tissue (Gerber et al., 2018). The molecular mechanism underlying the enrichment of Prrx1^{enh+} cells within mouse skin wounds is unknown, but live imaging of connective tissue during axolotl regeneration uncovered a pivotal role of cell migration in the process of blastema cell creation (Currie et al., 2016). It is tempting to think that activation of the *Prrx1* enhancer could relate to an increased readiness or propensity to migrate, which could relate to the role of *Prrx1* in epithelial to mesenchymal transitions (EMT) (Ocaña et al., 2012). In this study, we show that the protein expression of *Prrx1* differs from the activity of the 2.4kb upstream enhancer, and the results presented here argue for a subpopulation of enhancer versus PRRX1^{+} cells.

The heterogenous responses to healing by different fibroblastic populations is inarguably complex, and at least three sources could account for some aspects: 1) embryonic origin, 2) location in the body and 3) the microenvironment. One illustrating example is the different response to regeneration from fibroblasts in the P3 phalanx versus fibroblasts in the P2 phalanx (Wu et al., 2013).

In this work we investigated the response of *Prrx1* enhancer-expressing cells to injury and homeostasis. Because this enhancer is limb specific, we focused on full-thickness skin wounds in the limb. The majority of wound healing assays in murine models are based on back skin wounding due to the inaccessibility during grooming, the ability to make large wounds surpassing 5mm in diameter, and the possibility to splint (to mimic wound healing in humans where there is no contraction). The embryonic source of dorsal cells is diverse and could encompass cells from neural crest, pre-somitic mesoderm, and lateral plate mesoderm. In contrast, connective tissue of the limbs derives primarily from a single embryonic source of lateral plate mesoderm. In the future it will be interesting to assess if limb dermal cells display less heterogeneity compared to the dermal compartment of other regions that derive from diverse embryonic origins. In addition to being of a single embryonic source, experimental paradigms of wound healing in limbs have an important and clinical relevance for diabetic and trauma-related injuries.

One caveat of using a limb injury paradigm is that wound closure initiates by contraction of the skin. This limits a full comparison with data from splinted dorsal wounds. However, as our research focus is the ontogeny of limb progenitors, we set out to characterize wound healing in limb skin. In data not shown, we observed at 5 days post wounding a densely populated wound, scab formation and absence of blood vessels. By 21 days, the dermis is vascularized again and skin thickness has receded to almost half of the thickness at 14 days. We chose 14 days post wounding as a time where the wound is not fully resolved, but inflammation is decreased and the proliferative phase is winding down.

One of the most surprising results was the wide contribution of Prrx1^{enh+} cells to subcutaneous tissues under the wound bed. We administered Tamoxifen three weeks prior to wounding and never observed an enrichment of subcutaneous cells except in the context of wounding and did not observe a similar phenotype when labeling Col1a2^{enh+} fibroblasts. This suggests to us that Prrx1^{enh+} cells from the dermis immigrate into foreign subcutaneous tissues and contribute to adipocytes, fascia, and other structures. This resident tissue plasticity may be a conserved feature of Prrx1^{enh+} cells, since axolotl Prrx1^{enh+} cells are able to contribute to new segment formation in contrast to other mesenchymal cell populations (Gerber et al., 2018).

While Prrx1^{enh+} cells are able to expand and contribute to healing tissue, they do not seem to play a role in normal tissue growth and homeostasis as is the case for most epithelial stem cell pools. By labeling at several prenatal and early postnatal timepoints, we were unable to observe long term expansion of Prrx1^{enh+} clones that might arise from a tissue resident stem cell. Instead, Prrx1^{enh+} cells remained relatively quiescent during post-embryonic growth and restricted to the perivascular and dermal papilla niches. It was only post-injury that cells amplified during wound healing migration and proliferation. Our work suggests that Prrx1^{enh+} cells represent a specialized pool of injury-responsive cells. Recent work has highlighted similar populations of cells that are specifically tuned for tissue repair but not tissue maintenance and growth (Llorens-Bobadilla et al., 2015; Lopez-Baez, 2018; Marecic et al., 2015). It will be interesting in the future to understand what molecular factors drive the *Prrx1* enhancer during injury and to what degree they overlap with regulators of embryonic *Prrx1* enhancer activity. Based on the differences in *Prrx1* enhancer activity and PRRX1 protein expression, we believe that there are distinct molecular differences that differentiate enhancer-positive cells from the broader PRRX1 population which manifests in large differences in cell behavior during wound repair.

Overall, our results highlight that regenerative potential may not be lost but relegated to small minority of cells within adult tissue. As impressive as the response of Prrx1^{enh+} cells to injury, their

amplified numbers still make up only a small fraction of the overall population of wound fibroblasts. Future work aimed at understanding the molecular signals that retain and specify regenerative cells such as Prxx1^{enh+} cells will be key to tipping the balance from scar formation to regenerative tissue replacement.

Materials and Methods

Mouse Transgenesis

A construct was created containing the 2.4kb mouse *Prrx1* enhancer (REF) followed by the b-globin intron and nuclear-localized teal fluorescent protein-1 (mTFP1-nls), a T2A self-cleaving peptide, and CreERT2. The construct was linearized by digestion by KpnI and injected into the pro-nucleus of Bl6/J mouse oocytes (MPI-CBG Transgenic Core Facility). Six founder animals were generated and F1 progeny were screened for mTFP expression during embryonic limb development (E10.5-E12.5) and the ability to induce recombination of LoxP reporter lines only after administration of tamoxifen. From the initial founder animals, one line was further characterized and used for all subsequent experiments. All mouse lines were bred in MPI-CBG, CRTD and IMP facilities. All procedures performed in animals adhered to local ethics committee guidelines.

Mouse lines used in this manuscript:

Prrx1::mTFP1nls-T2A-CreERT2	This manuscript, MPI-CBG Transgenic Core Facility
B6;129S6-Gt(ROSA)26Sortm9(CAG-tdTomato)Hze/J	Jackson Labs stock # 007905
B6.129S4-Pdgfra<tm11 (EGFP) Sor>/J	Jackson Labs stock # 007669
K14.D2ΔNβ-cateninER	A kind gift from Fiona Watt, Ryan Driskell, and Makoto Mark Taketo
B6.Cg-Tg(Col1a2-cre/ERT,-ALPP)7Cpd/J	Jackson Labs stock #029567

Immunohistochemistry

Full thickness skin was dissected from mouse upper forelimb or lower back and attached to filter paper before submersing in 4%PFA in phosphate buffer. Tissue was fixed overnight at 4°C and then washed in PBS and serial overnight washes in 10% and 30% sucrose in PBS before being embedded in OCT and cryo-sectioned in longitudinal sections of 12 μm. For mouse limbs from E18.5 to 52 weeks of age, limbs were harvested and fixed overnight in PFA, washed in PBS, and incubated with 400 μM EDTA in PBS for approximately one week before washing in sucrose,

embedding and cryo-sectioning. Standard immunohistochemistry techniques were used for staining.

Antibodies used in this manuscript

Antibody	**Immunogen**	**Host**	**Source**
anti-PRRX1	axolotl	rabbit	Ocaña et al., 2017, MPI-CBG Antibody Facility
anti-SOX9	human	goat	R&D Systems
Anti-ALPHA SMOOTH MUSCLE ACTIN	human	rabbit	Abcam
anti-PERILIPIN	mouse	rabbit	Sigma-Aldrich
anti-CD31	mouse	rat	Dianova
anti-KERATIN 14	mouse	rabbit	Biolegend
anti-PRRX1	rat	rabbit	(Higuchi et al., 2013)

Tamoxifen administration

For recombination during embryonic limb development (E9.5-E12.5), pregnant females were given 1 mg of tamoxifen dissolved in corn oil by gavage approximately 24 hours prior to harvesting embryos. For adult recombination, animals were given 5x 5mg of tamoxifen by gavage every other day three weeks prior to wounding. Perinatal conversion constituted administration of 5 mg tamoxifen gavage starting at E19.5 to pregnant females and 2x 5mg gavage to mothers after birth.

Wounding

Animals were anesthetized by intraperitoneal injection of a mixture of Ketamine (100 mg/kg) and Xylazin (10 mg/kg). Skin was shaved, chemically defoliated, and wiped with 70% ethanol. To create a 2 mm wound in the forelimb, we pulled the skin from the posterior part of the limb (skin in the forelimb is not attached to the muscle-skeletal core) and at the crease, perforated with the half of a 2 mm punch biopsy. Wounds were immediately disinfected with iodine solution and wrapped with Tegaderm (3M) and bandage. Animals were given Carprofen at 4mg/kg and monitored during anesthetic recovery. Wounded animals were monitored daily for signs of infection and any self-removal of bandages. If animals had not removed forelimb bandages and

Tegaderm by two days post wounding, the dressing was manually removed to synchronize the kinetics of wound resolution. The wound in the posterior area of the limb ensured that the mice were not able to reach it and affect the healing process. Animals were sacrifice at either 5, 14, 21, or 28 days post wounding and skin was processed as described above.

Tissue dissociation and FACS

Animals were sacrificed and upper arm skin was shaved, and cut as full thickness skin. Adipose depots were manually removed, and the skin was washed once with 70% ethanol and three times with cold, sterile PBS. Skin was incubated in 10mg/ml elastase in DMEM at 37C° for 20 minutes. Dermal tissue was manually removed and separated from epithelial tissue. Dermal tissue pieces were then placed in xmg/ml Liberase TM in PBS with xUnits DNase for 37C° for 30 minutes and then manually dissociated by mechanical disruption with forceps to achieve a single cell suspension. Cell suspensions were filtered through a 50μm mesh and diluted in 10% serum containing DMEM. Cell suspensions were centrifuged at 900rcf and resuspended in serum-containing DMEM. Both filtered cells and unfiltered tissue pieces were plated on gelatin coated-tissue culture plates. 24 hours post-dissociation both filtered cells and unfiltered tissue were visually assessed for tdTOMATO expression. 24-48 hours after dissociation, cells were trypsinized, washed, and resuspended in FACs buffer containing 1x PBS (Ca/Mg free), 2 mM EDTA, 25 mM Hepes (pH 7.2), 1% BSA, and pen/strep. Non-transgenic controls skin was used to determine gating for tdTOMATO signal.

Imaging

Images were acquired with a 20x objective Apotome 2 (Zeiss) or inverted laser scanning confocal 780 (Zeiss) at 20 or 40x magnification. Imaging was performed on instruments of the Light Microscopy Facility, a core facility of CRTD at Technische Universität Dresden. Images were analyzed using Fiji and Photoshop, and alterations to brightness or contrast were applied equally to the entire micrograph for visualization purposes only. Cell quantification was performed in two sections per wound, of the mid area, of each animal. A region of interest measuring 1mm^2 was cropped in Fiji for quantification in both wound and contralateral, and samples were paired by animal to determine the fold increase. Statistical analyses were performed using the Graphpad Prism 7.0 software.

Author Contributions

JDC and TSG conceived and executed experiments, analyzed data, and wrote the manuscript. LG, MM and MS contributed experimental data and support. PM contributed the *Prrx1* enhancer construct and antibody. EMT and TSG secured funding for the project.

Acknowledgements

This work was supported by the animal facilities of the MPI-CBG, CRTD and IMP with institutional funding to EMT and TSG. EMT is supported by an ERC Advanced Grant. JDC acknowledges support from an EMBO Long Term Fellowship, Alexander Von Humboldt Fellowship, and MPI-CBG Fellowship. This work was supported by the Light Microscopy Facility, a core facility of BIOTEC/CRTD at Technische Universität Dresden. The authors are grateful to Yukio Kato's lab for kindly providing the anti-rat PRRX1 antibody. The authors claim no conflict of interest.

Figures

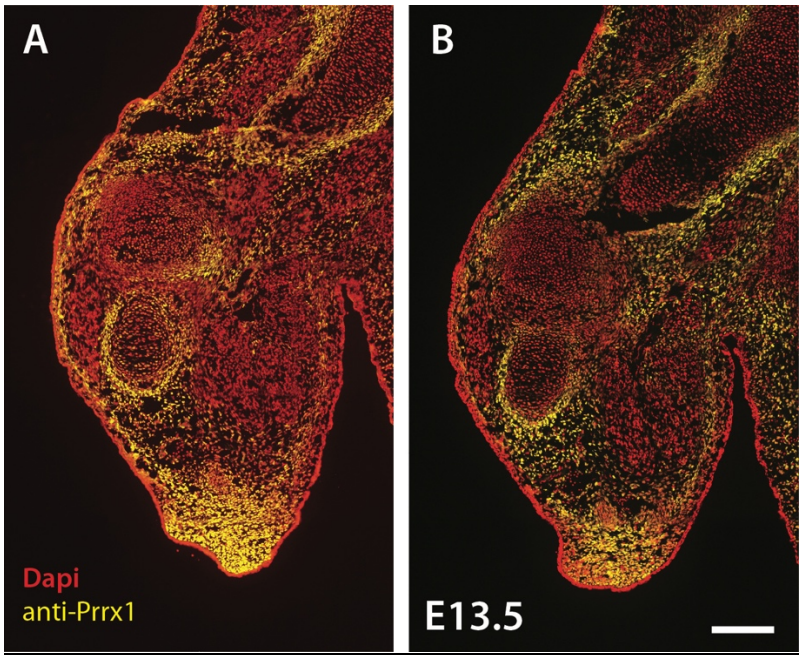

Figure 1. Anti-rat PRRX1 antibody vs our anti-axolotl PRRX1 in mouse sections.
(A) Staining of a E13.5 limb using an anti-rat PRRX1 antibody.

(B) In an immediate adjacent section, we tested our PRRX1 antibody. Our PRRX1 antibody recapitulates with fidelity the expression of the rat Prrx1 antibody. Scale bar, 200 microns.

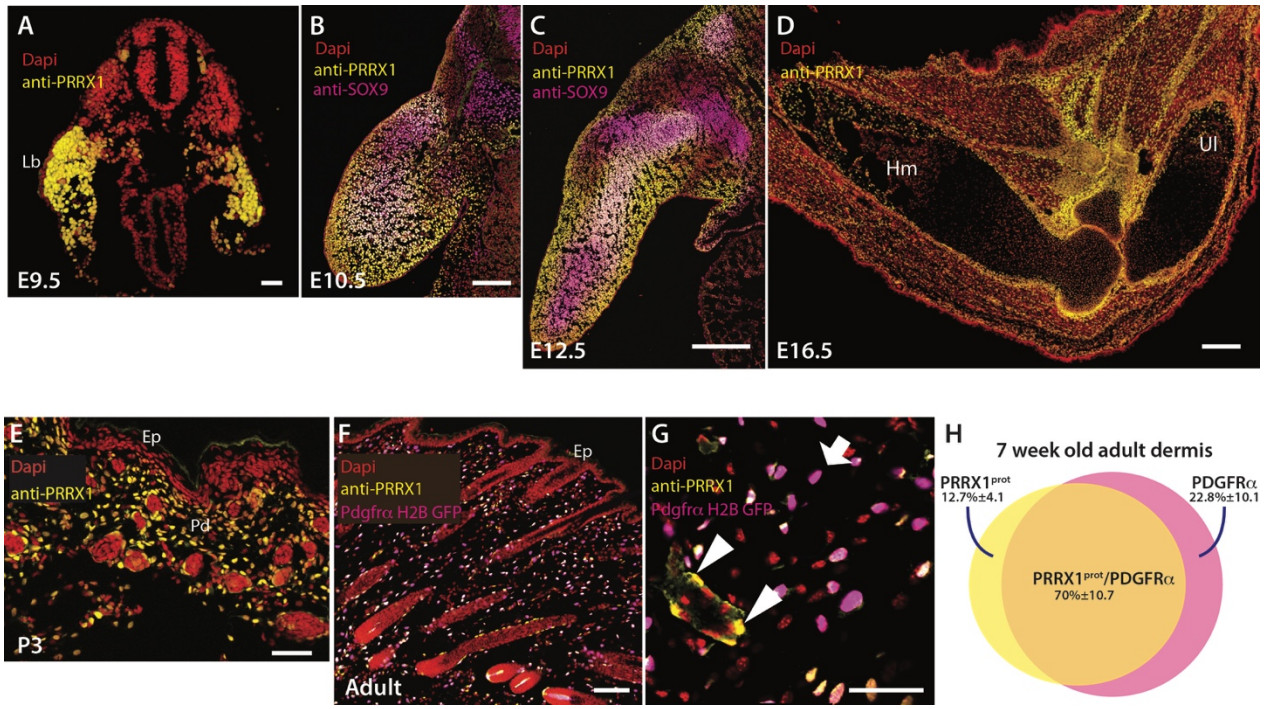

Figure 2. PRRX1 protein is abundantly expressed during limb development and in adulthood.

(A) Representative micrographs of antibody staining against PRRX1 protein. The peak of PRRX1 in the limb bud (Lb) is around embryonic day E9-10, nuclei is pseudocolored in red, PRRX1 antibody staining in yellow. Scale bar, 50 microns.

(B) At E10.5 cell condensations, positive for Sox9 protein (in magenta), in the midline of the limb down regulate Prrx1 protein expression. Scale bar, 200 microns.

(C) By E12.5, skeletal condensations are distributed along the limb and downregulated the PRRX1. Scale bar, 500 microns.

(D) At E16.5, the limb has patterned the musculo-skeletal elements Humerus (Hm), a clear elbow joint Ulna (Ul) and digits. PRRX1 is highest at the elbow area. Scale bar, 200 microns.

(E) After birth, at postnatal day 3 (P3), PRRX1^{+} cells are still present across dermis, including reticular and papillary dermis (Pd). Epidermis (Ep) is negative for PRRX1. Scale bar, 50 microns.

(F) In adult skin, PRRX1^{+} cells are compared to the population of cells PDGFRα^{+} (in magenta) and quantified (H). Scale bars (F) 200 microns,

(G) High magnification of adult skin. Arrows mark PDGFRα^{+} cells that are PRRX1^{-}. Arrowheads, PDGFRα^{-} cells that are PRRX1^{+}. Scale bar, 50 microns.

(H) Quantification of the PDGFRα and PRRX1 populations in adult dermis, represented in a Venn diagram. The mean percentage of cells/mm^{2} ± SD is reported.

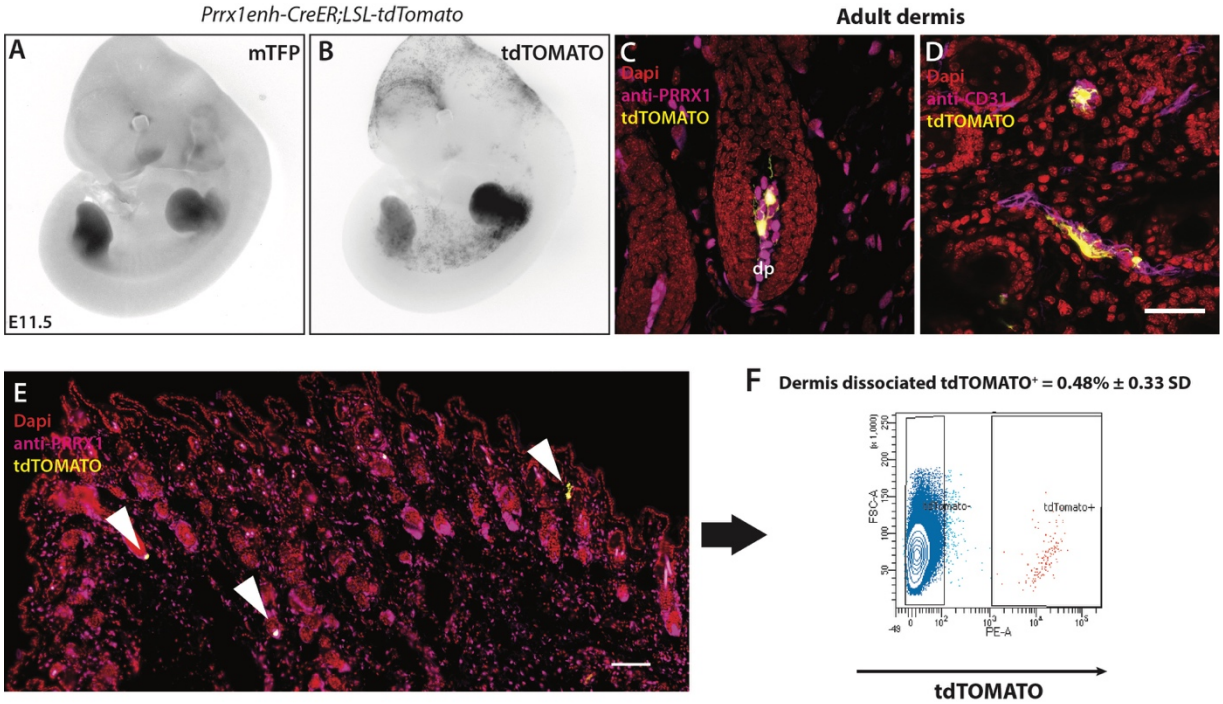

Figure 3. PRRX1 enhancer is active in limb bud mesenchyme progenitors and adult dermis.

To lineage trace the fate of Prrx1^{enh+} cells, a transgenic mice was created were *Prrx1 enhancer-CreER-T2A-mTFPnls* was crossed to a reporter line *Rosa-CAG-loxP-stop-loxP-TdTomato.* Referred to as *Prrx1enh-CreER;LSL-tdTomato*. (A) Inverted images of embryos showing limb TFP expression on E11.5 under the *prrx1* enhancer. (B) Upon tamoxifen administration, tdTOMATO^{+} (Prrx1^{enh+}) appear visible in limb bud. Additionally, Prrx1^{enh+} cells are present in a salt-and-pepper pattern in inter-limb flank, as well as cranial and craniofacial mesenchyme.

(C) (D) Prrx1^{enh+} cells in adult limb dermis. Cre recombinase activity labels cells mainly in dermal papilla (dp) and perivascular cells. Scale bar, 50 microns.

(E) An overview of the few labeled cells within the adult limb dermis. Arrow heads mark Prrx1^{enh+} positive cells. Scale bar, 200 microns.

(F) Dermal dissociation of cells three weeks after tamoxifen administration and FAC sorting of tdTOMATO^{+} cells, shows that in adult skin only a small population of cells retain the activity of the PRRX1 enhancer.

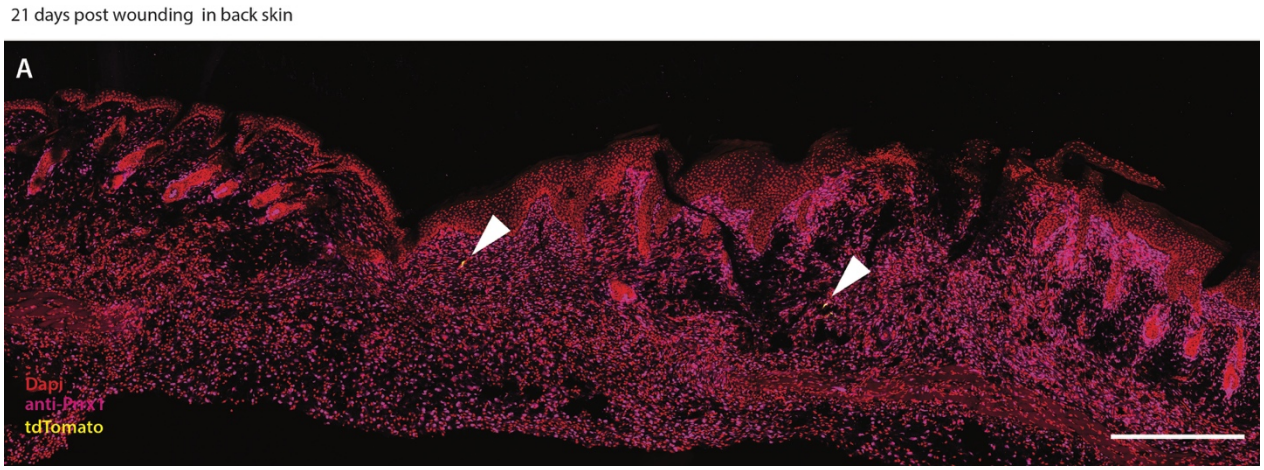

Figure 4. Back wounds are devoid of Prrx1^{enh+} cells.

(A) 2 mm full-thickness wounds in the dorsal trunk of *Prrx1enh-CreER;LSL-tdTomato* mice after 21 days. Scale bar, 500 microns.

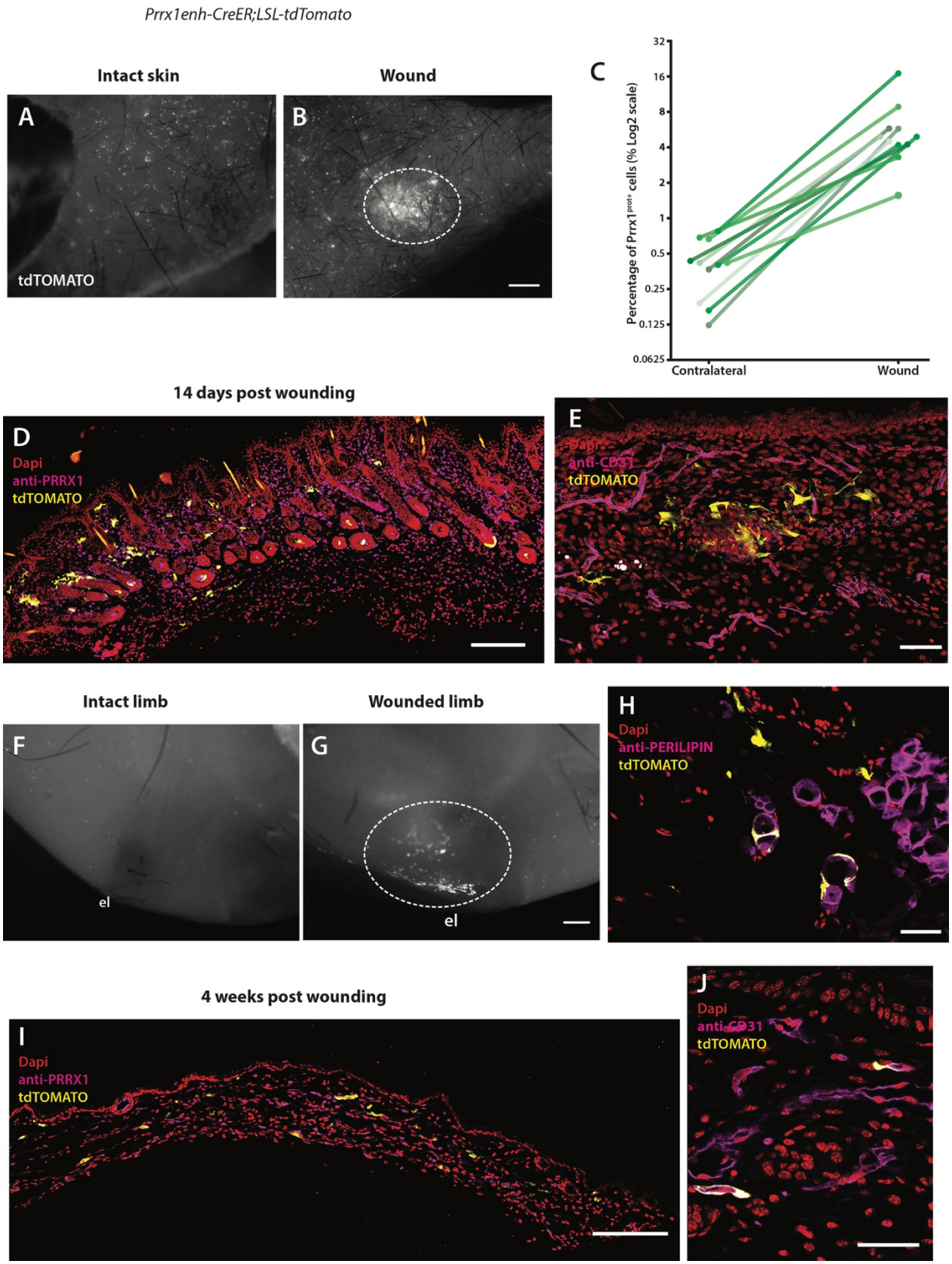
Prrx1enh-CreER;LSL-tdTomato
Intact skin
Wound
A
B
tdTOMATO
C
Percentage of Prrx1prot+ cells (% Log2 scale)
32
16
8
4
2
1
0.5
0.25
0.125
0.0625
Contralateral
Wound
14 days post wounding
D
Dapi
anti-PRRX1
tdTOMATO
E
Dapi
anti-CD31
tdTOMATO
Intact limb
Wounded limb
F
el
G
el
H
Dapi
anti-PERILIPIN
tdTOMATO
4 weeks post wounding
I
Dapi
anti-PRRX1
tdTOMATO
J
Dapi
anti-CD31
tdTOMATO

Figure 5. PRRX1 enhancer amplifies after injury in adult skin.

(A) Stereoscope micrograph of skin from an intact limb.

(B) Skin from wounded limb 21 days after wounding. Prrx1^{enh+} cells respond to 2 mm full thickness wounds in the limb, highlighted by dashed oval. Scale bar (A) and (B), 1mm.

(C) Quantification of Prrx1^{enh+} cells in sections from paired samples of contralateral and wounded limb skin. The percentage of Prrx1^{enh+} from the total PRRX1^{+} of cells/mm^2 $\pm$ SD are plotted. Y axis is shown in log2 for optimal visualization of values below 1.

(D) A representative skin section of a wound 21 days after wounding. Scale bar, 200 microns.

(E) Prrx1^{enh+} in wound bed. Cells are not associated to blood vessels during the resolving phase. Scale bar, 100 microns.

(F) Fixed limb of mouse after skin collection in contralateral limb; (el) elbow.

(G) Fixed limb of mouse after skin collection in wounded limb. Dashed oval marks the tissue under the wounded skin. Scale bar, 500 microns.

(H) Representative section of the limb connective tissue under the wound. In magenta PERILIPIN. Scale bar, 50 microns.

(I) At 4 weeks post wounding, inflammation has resolved and skin is thinner. Scale bar, 200 microns.

(J) At 4 weeks post wounding Prrx1^{enh+} return to be associated to blood vessels. Scale bar, 50 microns.

Long chase of Prrx1^{enh+}

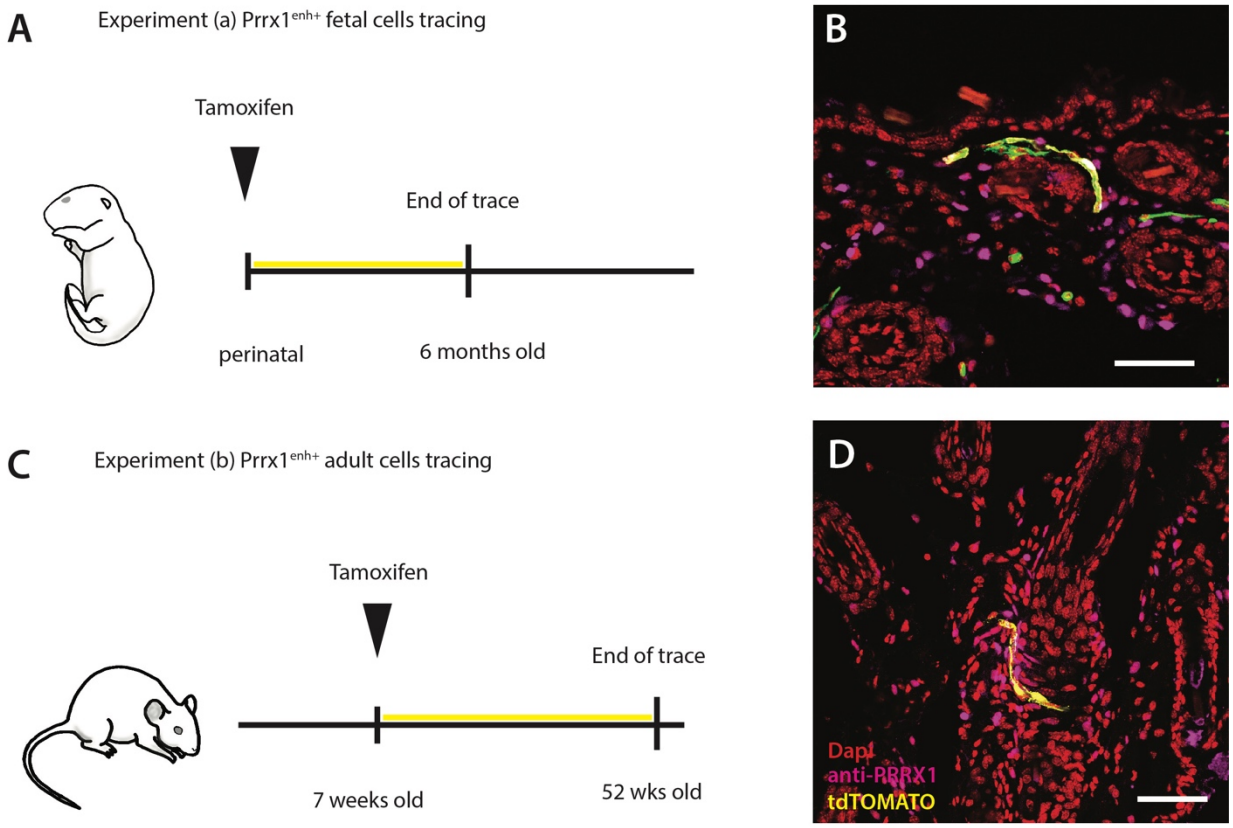

K14ΔNβ-cateninER;Prrx1-CreER;LSL-tdTomato

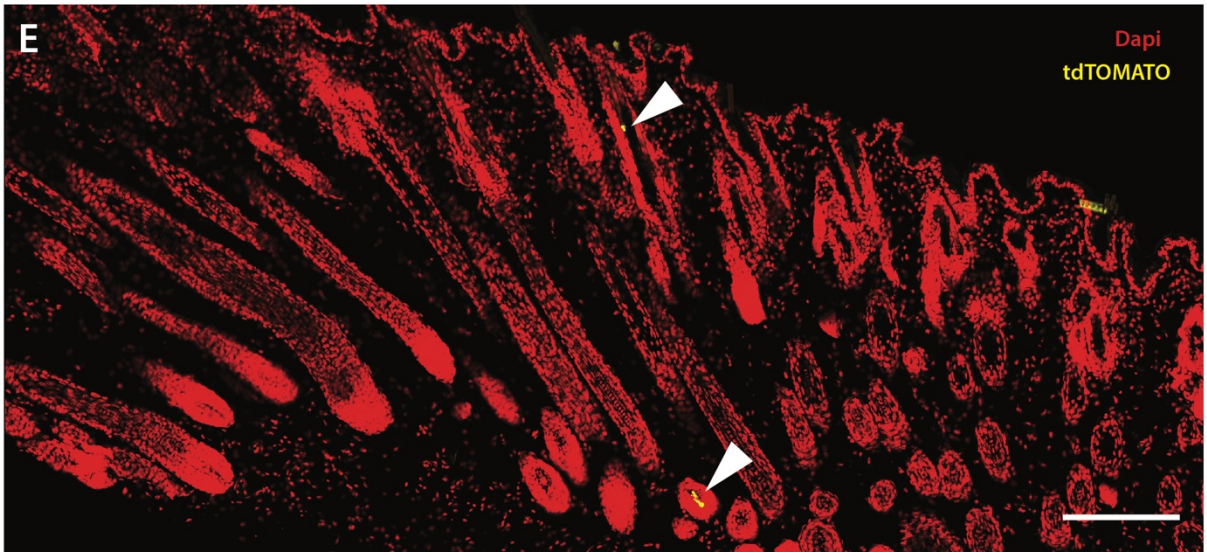

Figure 6. Perinatal and postnatal Prrx1^{enh+} don't play a role in dermis homeostasis.

(A) Graphic representation of experimental set up (a) to analyze the role of perinatal Prrx1^{enh+} cells in tissue homeostasis.

(B) A representative section of experiment (b) after 6 months. Scale bar, 50 microns.

(C) Graphic representation of experimental set up (b) to analyze the role of postnatal Prrx1^{enh+} in tissue homeostasis.

(D) A representative of experiment (a) after 1 year. Scale bar, 50 microns.

(E) The triple transgenic *K14**ΔN**β-cateninER;Prrx1enh-CreER;LSL-tdTomato* was used to bring the dermis to a neonatal state by sustaining the activity of Wnt/ *β*-catenin signaling. Three weeks after treatment, no difference in the number of Prrx1^{enh+} was found (arrowheads). Scale bar, 200 microns.

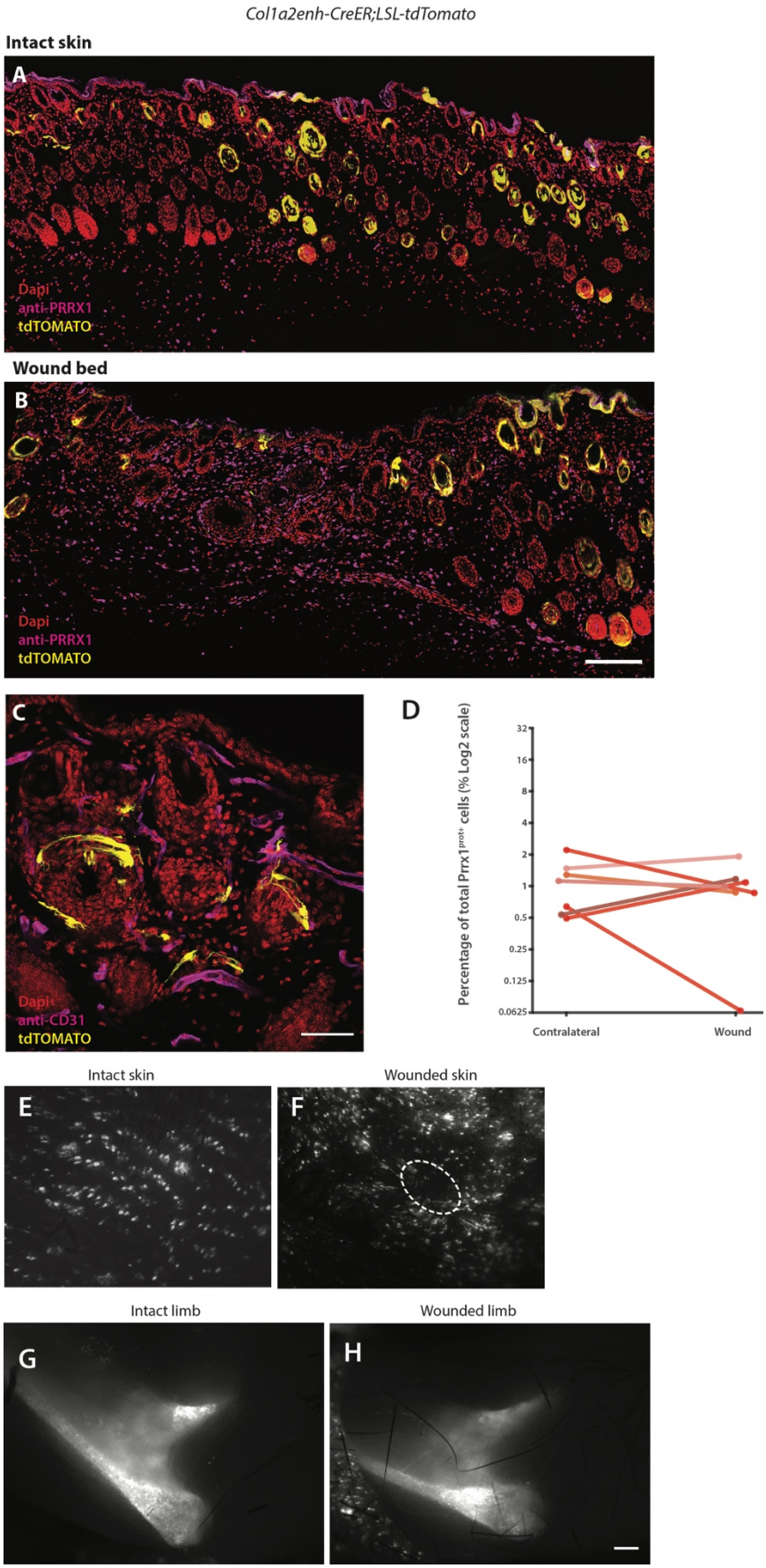
Col1a2enh-CreER;LSL-tdTomato
Intact skin
A
Dapi
anti-PRRX1
tdTOMATO
Wound bed
B
Dapi
anti-PRRX1
tdTOMATO
C
Dapi
anti-CD31
tdTOMATO
D
Percentage of total Prrx1prx1+ cells (% Log2 scale)
32
16
8
4
2
1
0.5
0.25
0.125
0.0625
Contralateral
Wound
Intact skin
Wounded skin
E
F
Intact limb
Wounded limb
G
H

Figure 7. COL1A2 enhancer does not amplify during wound healing.

(A) Intact skin of *Col1a2enh-CreER;LSL-tdTomato* mice 3 weeks after administration of tamoxifen. Scale bar, 200 microns.

(B) A 2 mm full thickness wounds in the posterior skin of the upper limb of *Col1a2enh-CreER;LSL-tdTomato.* Col1a2^{enh+} cells are mostly absent in the wound bed. Scale bar, 200 microns.

(C) Col1a2^{enh+} cells are not associated to blood vessels. Scale bar, 50 microns.

(D) Quantification of Col1a2^{enh+} cells in sections from paired samples of contralateral and wounded limb skin. The percentage of Col1a2^{enh+} from the total PRRX1^{+} of cells/mm^2 $\pm$ SD are plotted. Y axis is shown in log2 for optimal visualization of values below 1.

(E) Stereoscope micrograph of skin from an intact limb.

(F) Skin from wounded limb 21 days after wounding. Col1a2^{enh+} cells are mostly absent in 2 mm full thickness wounds in the limb, highlighted by dashed oval.

(G) Fixed limb of mouse after skin collection in contralateral limb.

(H) Fixed limb of mouse after skin collection in wounded limb. Positively labeled cells in the bone and skin and absent in connective tissue under the wounded dermis. Scale bar, 500 microns.

References

Chesterman, E. S., Gainey, G. D., Varn, A. C., Peterson, R. E., & Kern, M. J. (2001). Investigation ofPrx1 protein expression provides evidence for conservation of cardiac-specific posttranscriptional regulation in vertebrates. *Developmental Dynamics*, *222*(3), 459–470.

Collins, C. A., Kretzschmar, K., & Watt, F. M. (2011). Reprogramming adult dermis to a neonatal state through epidermal activation of β-catenin. *Development*, *138*(23), 5189–5199.

Currie, J. D., Kawaguchi, A., Traspas, R. M., Schuez, M., Chara, O., & Tanaka, E. M. (2016). Live Imaging of Axolotl Digit Regeneration Reveals Spatiotemporal Choreography of Diverse Connective Tissue Progenitor Pools. *Developmental Cell*, *39*(4), 411–423.

Demoulin, J.-B., Montano-Almendras, C. P. (2012). Platelet-derived growth factors and their receptors in normal and malignant hematopoiesis. *Am J Blood Res,* 1(2), 44-56.

Driskell, R. R., Lichtenberger, B. M., Hoste, E., Kretzschmar, K., Ben D Simons, Charalambous, M., et al. (2013). Distinct fibroblast lineages determine dermal architecture in skin development and repair. *Nature*, *504*(7479), 277–281.

Gerber, T., Murawala, P., Knapp, D., Masselink, W., Schuez, M., Hermann, S., et al. (2018). Single-cell analysis uncovers convergence of cell identities during axolotl limb regeneration. *Science*, 362(6413).

Gurtner, G. C., Werner, S., Barrandon, Y., & Longaker, M. T. (2008). Wound repair and regeneration. *Nature*, *453*(7193), 314–321.

Higashiyama, R., Nakao, S., Shibusawa, Y., Ishikawa, O., Moro, T., Mikami, K., et al. (2011). Differential Contribution of Dermal Resident and Bone Marrow–Derived Cells to Collagen Production during Wound Healing and Fibrogenesis in Mice. *Journal of Investigative Dermatology*, *131*(2), 529–536.

Higuchi, M., Kato, T., Chen, M., Yako, H., Yoshida, S., Kanno, N., & Kato, Y. (2013). Temporospatial gene expression of Prx1 and Prx2 is involved in morphogenesis of cranial placode-derived tissues through epithelio-mesenchymal interaction during rat embryogenesis. *Cell and Tissue Research*, *353*(1), 27–40.

Kramann, R., Schneider, R. K., DiRocco, D. P., Machado, F., Fleig, S., Bondzie, P. A., et al. (2014). Perivascular Gli1+ Progenitors Are Key Contributors to Injury-Induced Organ Fibrosis. *Stem Cell*, *16*(1), 1–17.

Kretzschmar, K., Cottle, D. L., Donati, G., Chiang, M.-F., Quist, S. R., Gollnick, H. P., et al. (2014). BLIMP1 Is Required for Postnatal Epidermal Homeostasis but Does Not Define a Sebaceous Gland Progenitor under Steady-State Conditions. *Stem Cell Reports*, *3*(4), 620–633.

Leussink, B., Brouwer, A., Khattabi, El, M., Poelmann, R. E., Gittenberger-de Groot, A. C., & Meijlink, F. (1995). Expression patterns of the paired-related homeobox genes MHox/Prx1 and S8/Prx2 suggest roles in development of the heart and the forebrain. *Mechanisms of Development*, *52*(1), 51–64.

Llorens-Bobadilla, E., Zhao, S., Baser, A., Saiz-Castro, G., Zwadlo, K., & Martin-Villalba, A. (2015). Single-Cell Transcriptomics Reveals a Population of Dormant Neural Stem Cells that Become Activated upon Brain Injury. *Stem Cell*, *17*(3), 329–340.

Logan, M., Martin, J. F., Nagy, A., Lobe, C., Olson, E. N., & Tabin, C. J. (2002). Expression of Cre Recombinase in the developing mouse limb bud driven by a Prx1 enhancer. *Genesis*, *33*(2), 77–80.

Lopez-Baez, J. C., Simpson, D. J., Lleras Forero, L., Zeng, Z., Brunsdon, H., Salzano, A., Brombin, A., et al. (2018). Wilms Tumor 1b defines a wound-specific sheath cell subpopulation associated with notochord repair. *eLife*, 7:e30657.

Marecic, O., Tevlin, R., McArdle, A., Seo, E. Y., Wearda, T., Duldulao, C., et al. (2015). Identification and characterization of an injury-induced skeletal progenitor. *Proceedings of the National Academy of Sciences*, *112*(32), 9920–9925.

Martin, J. F., & Olson, E. N. (2000). Identification of a prx1 limb enhancer. *Genesis*, 26, 225-229.

Mastrogiannaki, M., Lichtenberger, B. M., Reimer, A., Collins, C. A., Driskell, R. R., & Watt, F. M. (2016). β-Catenin Stabilization in Skin Fibroblasts Causes Fibrotic Lesions by Preventing Adipocyte Differentiation of the Reticular Dermis. *Journal of Investigative Dermatology*, *136*(6), 1130–1142.

Ocaña, O. H., Córcoles, R., Fabra, Á., Moreno-Bueno, G., Acloque, H., Vega, S., et al. (2012). Metastatic Colonization Requires the Repression of the Epithelial-Mesenchymal Transition Inducer Prrx1. *Cancer Cell*, *22*(6), 709–724.

Oliveira, C. R., Lemaitre, R., Murawala, P., Tazaki, A., Drechsel, D. N., & Tanaka, E. M. (2017). Pseudotyped baculovirus is an effective gene expression tool for studying molecular function during axolotl limb regeneration. *Developmental Biology*, *433*(2), 1–14.

Rajkumar, V. S., Shiwen, X., Bostrom, M., Leoni, P., Muddle, J., Ivarsson, M., et al. (2006). Platelet-derived growth factor-beta receptor activation is essential for fibroblast and pericyte recruitment during cutaneous wound healing. *The American Journal of Pathology*, *169*(6), 2254–2265.

Rinkevich, Y., Walmsley, G. G., Hu, M. S., Maan, Z. N., Newman, A. M., Drukker, M., et al. (2015). Skin fibrosis. Identification and isolation of a dermal lineage with intrinsic fibrogenic potential. *Science*, *348*(6232), aaa2151–2151-14.

Satoh, A., Gardiner, D. M., Bryant, S. V., & Endo, T. (2007). Nerve-induced ectopic limb blastemas in the Axolotl are equivalent to amputation-induced blastemas. *Developmental Biology*, *312*(1), 231–244.

Shi, Y., Bin Shu, Yang, R., Xu, Y., Xing, B., Liu, J., et al. (2015). Wnt and Notch signaling pathway involved in wound healing by targeting c-Myc and Hes1 separately. *Stem Cell Research & Therapy*, *6*(1), 1–13.

Shimozaki, K., Clemenson, G. D., & Gage, F. H. (2013). Paired related homeobox protein 1 is a regulator of stemness in adult neural stem/progenitor cells. *The Journal of Neuroscience : the Official Journal of the Society for Neuroscience*, *33*(9), 4066–4075.

Suzuki, M., Satoh, A., Ide, H., & Tamura, K. (2005). Nerve-dependent and -independent events in blastema formation during Xenopus froglet limb regeneration. *Developmental Biology*, *286*(1), 361–375.

Suzuki, M., Satoh, A., Ide, H., & Tamura, K. (2007). Transgenic Xenopus with prx1 limb enhancer reveals crucial contribution of MEK/ERK and PI3K/AKT pathways in blastema formation during limb regeneration. *Developmental Biology*, *304*(2), 675–686.

Wilk, K., Yeh, S.-C. A., Mortensen, L. J., Ghaffarigarakani, S., Lombardo, C. M., Bassir, S. H., et al. (2017). Postnatal Calvarial Skeletal Stem Cells Expressing PRX1 Reside Exclusively in the Calvarial Sutures and Are Required for Bone Regeneration. *Stem Cell Reports*, *8*(4), 1–24.

Wu, Y., Wang, K., Karapetyan, A., Fernando, W. A., Simkin, J., Han, M., et al. (2013). Connective Tissue Fibroblast Properties Are Position-Dependent during Mouse Digit Tip Regeneration. *PLoS ONE*, *8*(1), e54764.

Ye, J. Y., Chan, G. C. F., Qiao, L., Lian, Q., Meng, F. Y., Luo, X. Q., et al. (2010). Platelet-derived growth factor enhances platelet recovery in a murine model of radiation-induced thrombocytopenia and reduces apoptosis in megakaryocytes via its receptors and the PI3-k/Akt pathway. *Haematologica*, *95*(10), 1745–1753.

Yokoyama, H., Maruoka, T., Aruga, A., Amano, T., Ohgo, S., Shiroishi, T., & Tamura, K. (2011). Prx-1 Expression in Xenopus laevis Scarless Skin-Wound Healing and Its Resemblance to Epimorphic Regeneration. *Journal of Investigative Dermatology*, *131*(12), 2477–2485.